IX CONGRESSO BRASILEIRO DE
ENGENHARIA E CIÊNCIAS TÉRMICAS
9th BRAZILIAN CONGRESS OF THERMAL
ENGINEERING AND SCIENCES

Paper CIT02-0831

THE COMPLEX MOTION OF A GAS BUBBLE IN A NONLINEAR FLUID

Rodrigo Avelino Mesquita dos Santos
Departamento de Engenharia Mecânica - Universidade de Brasília
Campus Universitário Darcy Ribeiro - 70910-900 - Brasília - DF
rodrigo.avelino@bol.com.br

Francisco Ricardo da Cunha
Departamento de Engenharia Mecânica - Universidade de Brasília
Campus Universitário Darcy Ribeiro - 70910-900 - Brasília - DF
frcunha@unb.br

Aldo João de Sousa
Departamento de Engenharia Mecânica - Universidade de Brasília
Campus Universitário Darcy Ribeiro - 70910-900 - Brasília - DF
aldo@unb.br

Abstract. *The aim of this work is to examine the dynamical response of a spherical oscillatory bubble immersed in a suspension composed of a viscous fluid and anisotropic particles. These particles can be long fibers or macromolecules of high molecular weight. The bubble is composed of an ideal gas and it is set into motion growing and contracting in an acoustic pressure field. The effect of the hydrodynamic interaction between pairs of these particles for semi-dilute regime is investigated. Local orientation of the fibers is quantified by means of a probability density function. For a suspension of neutrally buoyant particles free of inertia and Brownian motion the local fiber orientation follows a Fokker-Planck equation. Numerical results of the bubble response to an acoustic pressure field are obtained for both situations: particles aligned to radial motion and for an initially random orientation of particles that involves in time. It is predicted that the addition of a low concentration of additives in an viscous fluid undergoing an acoustic pressure field may change significantly the nonlinear motion of collapsing bubbles*

Keywords: *additive suspension, oscillatory bubble, nonlinear motion*

1. Introduction

The study of the dynamics of gas bubbles in oscillating pressure field is of great interest in acoustic cavitation. The collapse of a bubble involves high pressure and temperature that may produce erosion in turbines, pumps, hydrofoils or propellers; emulsification; molecular degradation; biological effects; and, also, sonoluminescence and sonochemistry. These phenomena are subject of investigation in several works (e.g. Plesset and Prosperetti, 1977; Young, 1989; Hammit, 1980; Knapp et al., 1970; Barber et al., 1997).

Even with the assumption of sphericity the complete problem of a gas or vapor bubble undergoing nonlinear radial oscillations in a sound field is a complex flow. Besant, 1859 proposed a first equation to describe the motion of a spherical collapsing bubble. A more general study of bubble dynamics was developed by Rayleigh, 1917, who predict the time of collapse for an empty unbounded cavity immersed in a inviscid stationary fluid undergoing a pressure field. Rayleigh's theory found a collapse time $\tau = 0.915(\rho/p_0)^{1/2}R_0$, where ρ is is the fluid density, p_0 is the pressure field (constant) on the interface bubble-liquid and R_0 is the initial radius of the bubble. The fundamental equation of bubble dynamics was derived by (see, Plesset and Prosperetti, 1977) and it is known as the *Rayleigh-Plesset equation*

$$R\ddot{R} + \frac{3}{2}\dot{R}^2 = \frac{1}{\rho}\left[p(R,t) - p_\infty(t)\right]. \tag{1}$$

The dot denotes time derivative, $p(R,t)$ is the pressure in the liquid at the bubble wall, $p_\infty(t)$ is the pressure in the far field and R the radius of the bubble.

An analysis of the dynamics of spherical bubble that are perturbed away from an equilibrium volume by a finite amount has been reported for the case of a constant differential pressure by Cheng and Chen, 1986. Two relevant works that discuss the transitions of regular oscillations of the bubble radius to non-linear or chaotic oscillations were developed by Kameth and Prosperetti, 1989 and Szeri and Leal, 1991. The reader who is

interested in a comprehensive review of the predicted behavior of gas and vapor bubbles in time-dependent pressure fields should consult the excellent paper of Plesset and Prosperetti, 1977. An useful review of some researches on the dynamics of cavitation bubbles near boundaries is given by Blake and Gibson, 1987. More recently, Hao and Prosperetti, 1999 have examined the spherical dynamics of a vapor bubble in a oscillating pressure field by numerical simulations.

Acoustic cavitation is a strong incentive for the theoretical works on bubble dynamics. In this phenomenon the bubble motion is extremely non-linear and the bubble pulsations are not proportional to the acoustic excitation. Most of the previous work, however, were carried out analytically under severe restriction of linear or weakly nonlinear oscillations of a bubble in a Newtonian liquid. The corresponding problem for a gas bubble oscillating in a complex fluid is relatively new and much less developed, and the effect of a low concentration of suspending anisotropic particles on the non-linear response of a oscillating bubble is still poorly understood.

The purpose of this work is a theoretical investigation of the response of a gas bubble immersed in a dilute suspension of anisotropic additives undergoing a transient pressure field. The additives can be long fibers or else polymeric macromolecules of high molecular weight. An extension of Eq.(1) is developed to study this problem. The effect of hydrodynamics interaction between pairs of additive for semi-dilute regime is explored and local orientation of the particles is quantified by means of a probability density function. The Reynolds number (Re), the Weber number (We) and the additives concentration and aspect ratio are the most important parameters for describing the physics of bubble oscillatory motion in such complex fluid. We examine the effect of additives on the non-linear motion of a bubble. The history of the bubble motion, phase diagrams and diagrams of collapse will be determined by our analytical expressions and numerical integrations.

2. Description of the problem

Consider an ideal gas filling a bubble of initial radius R_0 developing an oscillatory motion in an semi-dilute suspension. The suspension is composed of cylindrical fibers or polymeric molecules of aspect ratio ℓ/a and volume fraction ϕ and an incompressible Newtonian fluid of viscosity μ and density ρ. The internal gas describes a polytropic process $p_b V^n = constant$, where p_b is the internal absolute pressure, $V = (4/3)\pi R^3$ is the bubble volume at any time and n is the polytropic coefficient. It is assumed that the bubble remains perfectly spherical and thus the bubble surface $r = R(t)$ moves only in the radial direction. It is also supposed spatially uniform conditions within the bubble; that no body forces are present, that the density of the liquid is large; the compressibility small and that the properties of gas inside the bubble constant. The bubble in the suspension is excited by the acoustic perturbation $p_\infty(t) = p_0(1 + \varepsilon \sin \omega t)$. Here ε is the pressure amplitude and ω its frequency. Figure (2) illustrates the model.

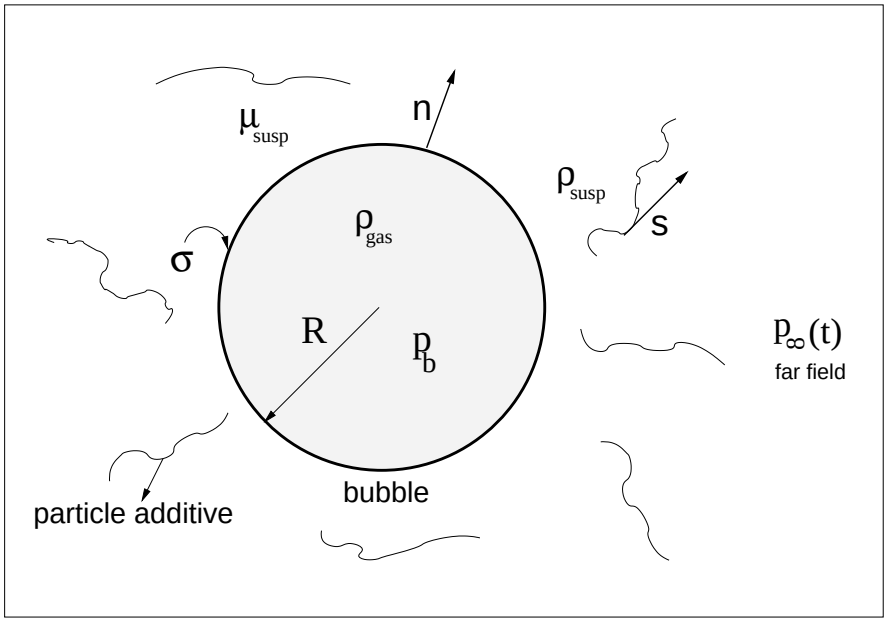

Figure 1: Schematic of a spherical bubble in a additive suspension under a variable pressure field

3. Mathematical formulation

Now an extension of the *Rayleigh-Plesset* equation (1) is derived here taking into account effects such as surface tension, the extensional viscosity of the suspension related to the additives and the acoustic pressure forcing.

3.1. Balance equations

Owing to the pure radial motion of the bubble and the incompressibility of the suspension flow, the continuity equation in spherical coordinates reduces simply to

$$\frac{1}{r^2}\frac{\partial}{\partial r}(r^2 u) = 0. \tag{2}$$

Here r is the distance from the bubble center to an arbitrary point in the external fluid, and u is the radial component of the velocity. Integrating the above equation and applying the kinematic boundary condition $u(r = R, t) = \dot{R}$, one obtains

$$u(r,t) = \frac{R^2}{r^2}\dot{R} \tag{3}$$

The general balance momentum is given by the Cauchy's equation:

$$\rho\left(\frac{\partial \mathbf{u}}{\partial t} + \mathbf{u}\cdot\nabla\mathbf{u}\right) = \nabla\cdot\boldsymbol{\Sigma} + \rho\mathbf{g}, \tag{4}$$

where $\boldsymbol{\Sigma}$ is the fluid stress tensor, $\mathbf{u}$ is the velocity field and $\mathbf{g}$ is the gravity acceleration vector.

3.2. Constitutive equations for the stress tensor

The stress tensor $\boldsymbol{\Sigma}$ in Eq. (4) cannot be described by a Newtonian model because the presence of additive causes a stress anisotropy in the flow. We follow the same constitutive model of our previous work (Santos and Cunha, 2001) for a suspension of anisotropic particles.

$$\boldsymbol{\Sigma} = -p\boldsymbol{I} + 2\mu\boldsymbol{D} + 2\boldsymbol{\Sigma}^f, \tag{5}$$

where p is the pressure on the system, $\boldsymbol{I}$ is the isotropic unity tensor, $\boldsymbol{D}$ is the rate of strain tensor, $\boldsymbol{D} = \frac{1}{2}\left(\nabla\boldsymbol{u} + (\nabla\boldsymbol{u})^T\right)$ where T denotes to the transpose operation of $\nabla\boldsymbol{u}$ and $\boldsymbol{\Sigma}^f$, the stress tensor due to the additives, was based on a particular case of the general formulation proposed by Hinch and Leal, 1970 in which a additive suspension of particles free of inertia, sedimentation and Brownian motion is taken into account. Thus, the additive contribution on the stress tensor can be written as

$$\boldsymbol{\Sigma}^f = \mu_e(\mathbf{s}\cdot\mathbf{D}\cdot\mathbf{s})\mathbf{ss}, \tag{6}$$

Physically, $\boldsymbol{\Sigma}^f$ corresponds to an extra stress in the direction of the additive orientation $\boldsymbol{s}$ that is proportional to the rate of strain tensor component $\boldsymbol{s}\cdot\boldsymbol{D}\cdot\boldsymbol{s}$. A polymeric macromolecule or a long fiber tends to resist to the stretching along its own axis and the extensional viscosity μ_e characterizes the importance of this resistance. Figure (2) illustrates the non-linear model proposed.

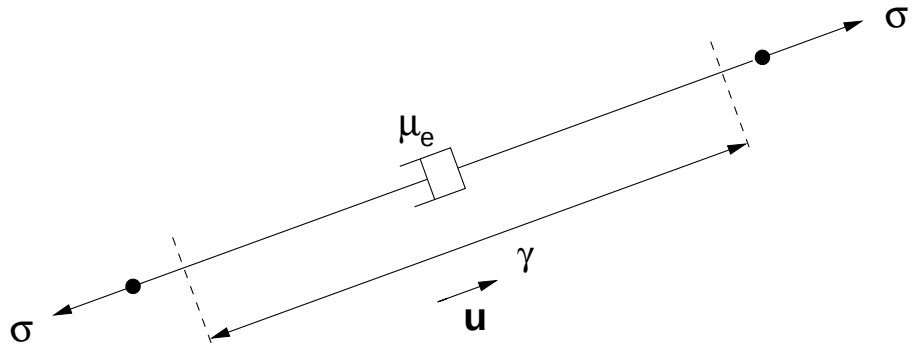

Figure 2: Non-linear model of extensional viscosity

3.3. Boundary conditions at the interface

In a clean interface (free of surfactants), there is velocity and tangential stress continuity, but normal stress discontinuity (normal stress jump) on the bubble-suspension interface. These boundary conditions can be expressed as

$$(\sigma_{tt})_{susp} = (\sigma_{tt})_{gas} \tag{7}$$

$$u_{susp} = u_{gas} \tag{8}$$

$$\sigma_{nn} = (\boldsymbol{n} \cdot \boldsymbol{\Sigma} \cdot \boldsymbol{n})_{susp} - (\boldsymbol{n} \cdot \boldsymbol{\Sigma} \cdot \boldsymbol{n})_{gas} = 2K\sigma \tag{9}$$

The subscripts *susp* and *gas* denote, respectively, the traction in the suspension side and in the gas side. Here $\sigma_{tt} = \boldsymbol{t} \cdot \boldsymbol{\Sigma} \cdot \boldsymbol{t}$, $\boldsymbol{t}$ is the unitary vector tangent to the bubble surface, $\boldsymbol{n}$ is the normal unitary vector, σ is the surface tension coefficient and $\bar{K} = \frac{1}{2}\left(\frac{1}{R_1} + \frac{1}{R_2}\right)$ is the mean curvature of the bubble surface. As the bubble remains spherical and oscillating in radial motion, the mean curvature reduces to $1/R$.

The normal stress inward the bubble is given as

$$(\mathbf{n} \cdot \boldsymbol{\Sigma} \cdot \mathbf{n})_{gas} = -p_g \left(\frac{R_0}{R}\right)^{3n}, \tag{10}$$

and developing the stress tensor given in Eq. (5) the traction component outwards the bubble can be written as

$$(\mathbf{n} \cdot \boldsymbol{\Sigma} \cdot \mathbf{n})_{susp} = -p(R,t) - 4\mu\frac{\dot{R}}{R}\langle f(\phi, \ell/a, R, \theta)\rangle. \tag{11}$$

Substituting Eq. (10) and (11) in Eq. (9) and considering equilibrium at the initial instant Santos and Cunha, 2001 has found that the pressure of the gas inside the bubble and the pressure in the suspension side are given, respectively, by

$$p_b^*(R,t) = \left(p_0 + \frac{2\sigma}{R_0}\right)\left(\frac{R_0}{R}\right)^{3n}. \tag{12}$$

$$p(R,t) = \left(P_0 + \frac{2\sigma}{R_0}\right)\left(\frac{R_0}{R}\right)^{3n} - \frac{2\sigma}{R} - 4\mu\frac{\dot{R}}{R}\langle f(\phi, \ell/a, R, \theta)\rangle. \tag{13}$$

$\langle f(\phi, \ell/a, R, \theta)\rangle$ defined below refers to the presence of additives in the fluid outward the bubble. This rheological function can be expressed, for a general case, as a function of the suspension and flow parameters: the aspect ratio and concentration of particles

$$f\,(\phi, \ell/a, R, \theta) = \left(1 + \frac{\mu_e}{\mu}\cos^4\theta\right) \tag{14}$$

Notice that θ is the local orientation of the particles in relation to the radial direction. The average effect of the extensional viscosity on the rheology of the suspension is related to the probability average of f since θ is the local orientation of the particle. Thus,

$$\langle f\rangle = 1 + \frac{\mu_e}{\mu}\int_{-\infty}^{\infty}\int_{-\infty}^{\infty}\cos^4\theta P(r,\theta)drd\theta \tag{15}$$

where $P(r,\theta)$ is a probability density function related to the orientation of the particles in the suspension. For convenience we define a function that takes into account the orientation of the additives, we have

$$G(\theta) = \int_0^{2\pi}\int_R^{\infty}\cos^4\theta P(r,\theta)drd\theta \tag{16}$$

3.4. Bubble dynamics governing equation

Finally, the extension of Eq. (1) considering all the parameters of the system studied

$$R\ddot{R} + \frac{3}{2}\dot{R}^2 = \frac{1}{\rho}\left(p_0 + \frac{2\sigma}{R_0}\right)\left(\frac{R_0}{R}\right)^{3n} - \frac{2\sigma}{\rho R} - \frac{4\mu\langle f(\phi,\ell/a)\rangle}{\rho}\frac{\dot{R}}{R} - \frac{p_\infty(t)}{\rho}. \tag{17}$$

Making a simple change of variable of the type

$$R = R_0(1+r) \qquad \text{and} \qquad p_\infty(t) = p_0(1+p^{'}(t)), \tag{18}$$

and after non-dimensionalization of the problem using the appropriate scalings

$$u_c = \left(\frac{p_0}{\rho}\right)^{1/2}; \qquad R = R_0 \qquad \text{and} \qquad \tau_c = \frac{R_0}{(p_0/\rho)^{1/2}}. \tag{19}$$

The dimensionless governing equation is found to be

$$\begin{aligned}(1+r)\ddot{r} + \frac{3}{2}\dot{r}^2 &= \frac{2}{We}\left[\frac{1}{(1+r)^{3n}} - \frac{1}{(1+r)}\right] - \\ &- \frac{4}{Re}\left(1 + \langle f(\phi,\ell/a,R)\rangle\right)\frac{\dot{r}}{(1+r)} - (1+p^{'}(t)) + \frac{1}{(1+r)^{3n}},\end{aligned} \tag{20}$$

with the dimensionless equation for the gas pressure (p_b) given by

$$p_b(t) = \left(1 + \frac{2}{We}\right)R(t)^{-3n}. \tag{21}$$

In Eq. (20) and Eq. (21) the relevant physical parameters are: the Weber number (We) and the Reynolds number (Re). Both can be defined after a simple scaling argument. If $F_i \sim \rho R_0^2 U_c^2$ is the inertial force, $F_\mu \sim \mu R_0 U_c$ is the viscous force and $F_\sigma \sim R_0\sigma$ is the surface tension force, we define We as F_i/F_σ and Re as F_i/F_μ.

3.5. Material function for suspension of aligned particles

All the functions determined in this section has been determined using the hypothesis of additives aligned to the flow direction in any instant. The slender-body theory of Batchelor, 1970 gives an expression to the function $(\phi,\ell/a)$ for dilute suspension

$$f(\phi,\ell/a) = 1 + \frac{4}{3}\phi\frac{(\ell/a)^2}{\ell n(\ell/a)}. \tag{22}$$

A correction for semi-dilute regime has been proposed and can be found in Hinch and Cunha, 1997. It leads to

$$f(\phi,\ell/a,R) = 1 + \frac{4}{3}\phi\frac{(\ell/a)^2}{\ell n\phi^{-\frac{1}{2}}}. \tag{23}$$

Two corrections of the above functions are also considered ($F(\alpha)M(\phi)f(\phi,\ell/a,R)$). The shape factor function $F(\alpha)$, derived by Batchelor, 1971 corrects both Eq. (22) and Eq. (23) for finite aspect ratio of the additives. This function is equal to 1 for infinitely long particles. It is given as

$$F(\alpha) = \frac{1+0.64\alpha}{1-\frac{3}{2}\alpha} + 1.659\alpha^2 + O(\alpha^2), \tag{24}$$

where $\alpha = [\ell n(\ell/a)]^{-1}$.

An expression for inter-particle interactions derived by Shaqfeh and Frederickson, 1990 takes into account the effect of two-particle hydrodynamic interaction on the equivalent viscosity for semi-dilute regime. This correction is given by

$$M(\phi) = \left[\ell n\left(\frac{1}{\phi}\right) + \ell n\left(\ell n\left(\frac{1}{\phi}\right)\right) + E(\phi)\right]^{-1}, \tag{25}$$

where $E(\phi)$ is of order 1 in the limit $\phi \to 0$. For aligned cylindrical particles Shaqfeh and Frederickson, 1990 found that $E(\phi) = 0.1585$.

3.6. A model for a suspension of random oriented additives

The local orientation of a single fiber or macromolecule in relation to the local radial direction, θ is determined by means of the probability function $P(\theta)$. The common models for the material function given in Eq. (14) consider particles aligned in the flow direction (Shaqfeh and Frederickson, 1990). In this section it is proposed a model that takes into account additives randomly oriented in the suspension. The probability density function of the Eq. (16) must be known to proceed with the analysis of the rheological extensional function. In this model we consider that that motion of the bubble does not make any effect influence on the initial particle orientation distribution. In other words, $P(r,\theta) = P(\theta)$. It is proposed here that the additives are randomly oriented in whole suspension domain. Thus the orientation particle distribution follows a Gaussian probability density as $P(\theta) = N(\bar{\theta}, \sigma_\theta^2)$ in which $\bar{\theta}$ is the mean orientation of the particles and σ_θ is the associated standard deviation.

$G(\theta)$ that calculates the rheology of the suspension of randomly oriented particles is written as follow

$$G(\theta) = \int_0^{2\pi} \cos^4\theta \frac{1}{\sigma_\theta\sqrt{2\pi}} e^{-(\theta-\bar{\theta})^2/2\sigma_\theta^2} d\theta. \tag{26}$$

Notice that for $\theta = 0 \ \forall \ t$, $G(\theta) = 1$, recovering the Eq.(22).

4. Numerical integration

A fourth order Runge-Kutta scheme has been used to obtain the numerical solution of the initial value problem. We use the Lahey Fortran 95 in Conectiva Linux 6.0 on a Pentium III, 900 MHz cell. As a test of the numerical code, the collapse time given by Rayleigh theory was verified. It was used a time step equal to 10^{-3} and the simulation error was much smaller than 1%. It should be important to note that the bubble collapse occurs when it reaches the limit of maximum packaging of the gas molecules. This incompressible limit is called van der Walls *hard core*. According to Knapp et al., 1970, if the gas is air, the dimensionless minimum radius is around 0.1.

Time evolution of the bubble motion is obtained for several set of the parameters of the system (We, Re, pressure amplitude, aspect ratio and concentration of additives). Collapse diagrams (Re $\times$ We) are plotted in order to show the range the bubble collapses or not. The influence of the additives is also explored through the collapse diagrams.

The bubble response in a suspension of aligned particles, $\theta = 0 \ \forall \ t$, is compared to its oscillations in a suspension of randomly oriented additives. The results here are obtained several values of $\bar{\theta}$ and σ_θ. A study of the rheology of the suspension is also showed. The solution of $G(\theta)$ is obtained numerically by trapezoidal rule.

5. Results and discussion

In following, it is presented some numerical results for several sets of the parameters of the system. The influence of the fibers in the flow is characterized. Firstly, it is shown some plots of the nonlinear motion of the bubble. Despite the fact that the bubble, in some cases do not reaches the collapse the oscillatory motion is extremely unstable.

The nonlinear response of a spherical bubble developing a pure radial motion in absence of additives ($\phi = 0$) is shown in Fig (3). The bubble is set into motion in a pressure field of amplitude $\varepsilon = 1.5$. The Reynolds number and the Weber number of this flow are equal to 7. It is seen that the bubble motion is not harmonic in a period of oscillation.

Notice that the radius of the bubble does not oscillate as the pressure (p_∞) forcing does, in other words its dynamic is not proportional to the pressure input. The plot (b) in Fig.(3) corresponds to the phase diagram of the bubble motion. It shows the velocity of the bubble interface as a function of the bubble radius. The figure becomes more deformed as more unstable the flow. If we have a stable motion the diagram tends to form a circle, in other words a phase diagram is good way to describe the flow stability.

In Fig. (4) it is shown a critical cavitation that carries the bubble to the collapse. In this plot $Re = 30$, $We = 30$, the pressure amplitude is $\varepsilon = 1.5$ and there is no additive particle in the outwards fluid. The bubble reaches the *van der Walls hard core* before it complete one period of oscillation (see (a)). Note that soon after the bubble reaches the maximum radius it starts to contract rapidly and collapses when t is approximately 15. It is seen that the pressure input variation is smooth in contrast to the bubble motion. In general the results show a phenomenon strongly non-linear in which the bubble response does not follow the harmonic oscillations of the acoustic ambient pressure. In (b) the phase diagram is opened due to the collapse.

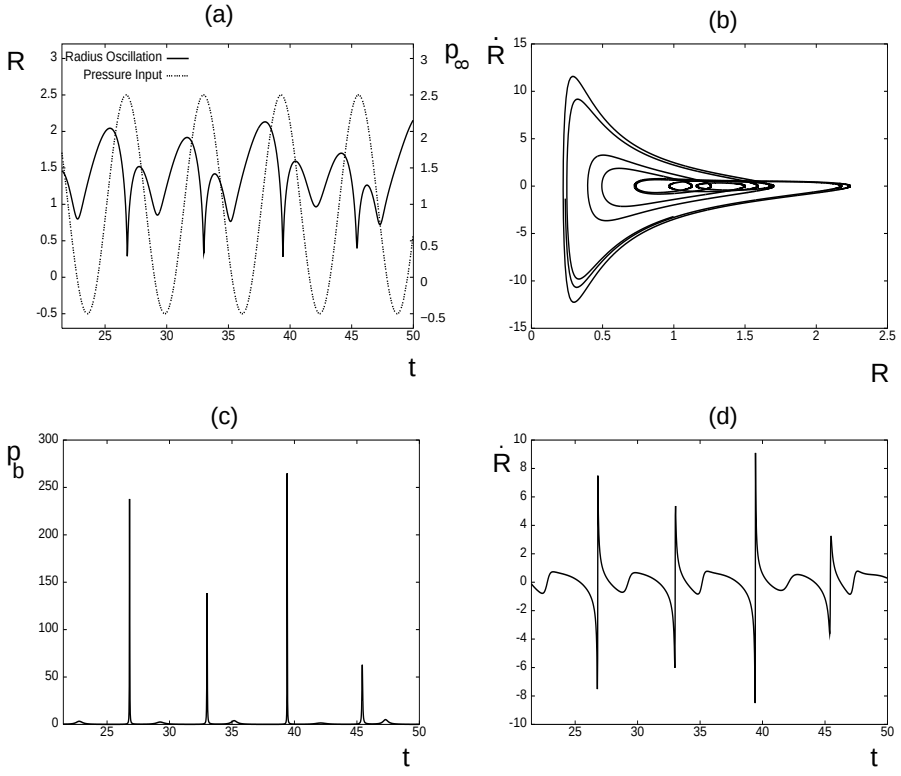

Figure 3: Time developing of the oscillatory motion of a bubble. $Re = 7$, $We = 7$, $\varepsilon = 1.5$ and $\phi = 0$. (a) is the radius of the bubble (full line) and the pressure input (dot line) as a function of time; (b) shows the phase diagram ($\dot{R} \times R$).

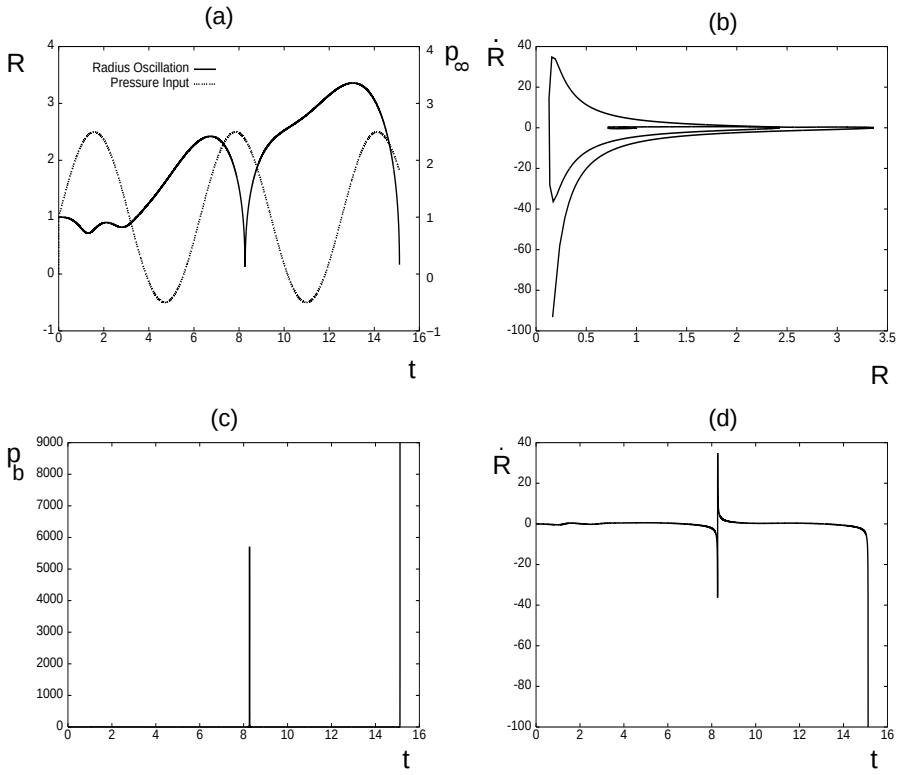

Figure 4: Time developing of the oscillatory motion of a bubble. $Re = 30$, $We = 30$, $\varepsilon = 1.5$ and $\phi = 0$. (a) is the radius of the bubble (full line) and the pressure input (dot line) as a function of time; (b) shows the phase diagram ($\dot{R} \times R$).

5.1. Aligned additives influence in the flow

In this section, a small concentration of particles is added to the external liquid and the bubble develops its motion in a non-Newtonian suspension of anisotropic particles.

Fig (5) shows the oscillations for $Re = 30$, $We = 30$, $\varepsilon = 1.5$ (same conditions of plot in Fig (4)) and a low concentration of additives (ϕ) equal to 0.01 with aspect ratio 100.

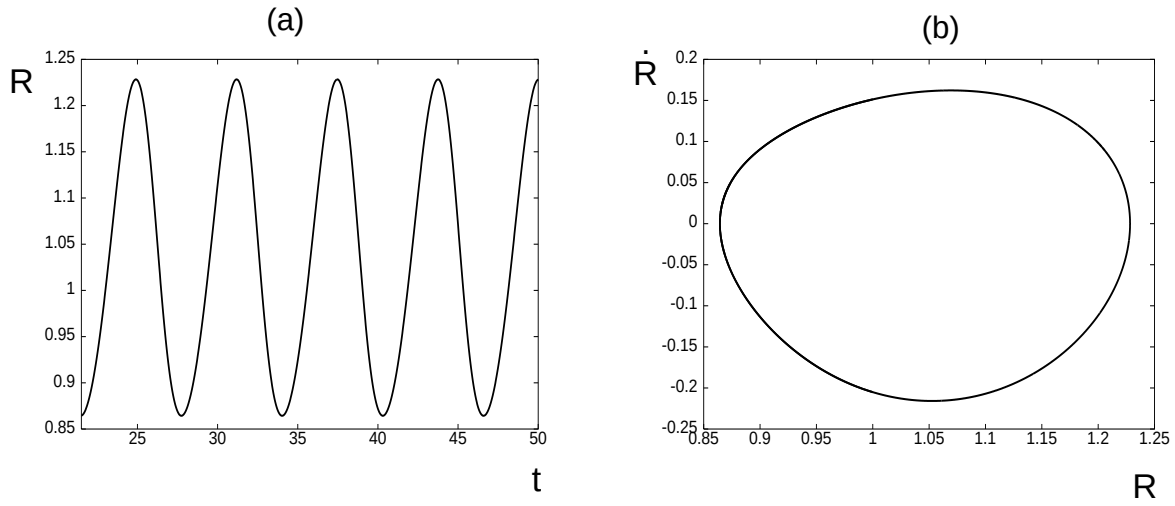

Figure 5: The additive effects on the dynamic of a oscillatory bubble. $Re = 30$, $We = 30$, $\varepsilon = 1.5$, $\phi = 0.01$ and $\ell/a = 100$. (a) is the radius of the bubble (full line) and the pressure input (dot line) as a function of time; (b) shows the phase diagram ($\dot{R} \times R$).

In contrast with the behavior observed in Fig (4), it is seen even for low values of volume fraction ϕ, the bubble motion is stabilized and it oscillates approximately with the same frequency of the forcing pressure, but not in phase. The phase diagram is slightly deformed, i.e. the motion is not exactly harmonic. However, even in a critical situation fibers or polymeric macromolecules may become the flow stable.

A collapse diagram (Re as a function of We) is a plot that shows the collapse and non-collapse regions for a set of the geometrical parameters of the additives (ϕ and aspect ratio). In absence of the additive particles and for $\varepsilon = 1.5$, Fig (6) shows the collapse diagram. There is a small non-collapse region in the range of $0 < We < 80$ and $0 < Re < 80$. The line of the diagram represents the collapse threshold. The region upper this line is the collapse one. The non-collapse regions is for values lower than Reynolds number around 9 and for We around 2 . Thus, the stability of the system is more sensitive to variations in Reynolds number rather than to Weber numbers.

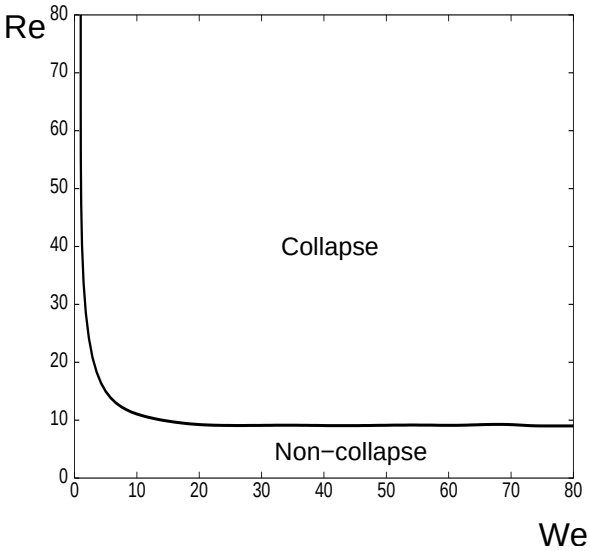

Figure 6: Collapse diagram. $\phi = 0$ and $\varepsilon = 1.5$

The effect of additives may be observed by means of a collapse diagram. Figure (7) shows, for fixed values

of the aspect ratio, the variations of the collapse region as a function of the additives concentration. In (a) $\ell/a = 80$ and in (b) $\ell/a = 120$. In both computations, the non-collapse region increase as just a small addition of anisotropic particles in the flow, Typically for $\phi = 0.0005$ the critical Reynolds number changes from 10 to about 20 for $\ell/a = 80$ and to 30 for $\ell/a = 120$. In the plateau region for $We = 40$ $Re_c(\phi = 0.0005)$ is equal to around 18 and $Re_c(\phi = 0.001)$ is equal to approximately 30 in Fig (7(a)).The effect of elongation of the particles is more pronounced for longer particles. This effect tends to inhibit the high amplitudes of the motion. The results show that more flexible particles (high aspect ratios) tends to linearize more the oscillations. If the aspect ratio is increased the collapse threshold occurs for higher Reynolds number.

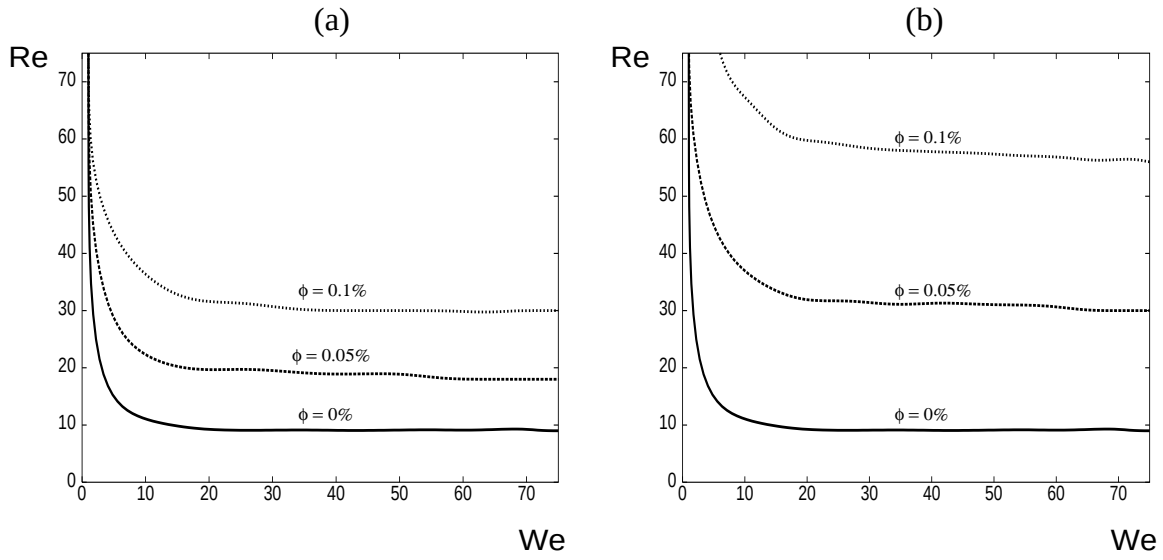

Figure 7: Collapse diagram for fixed aspect ratio. (a) $\ell/a = 80$ and (b) $\ell/a = 120$

5.2. Influence of geometrical parameters and inter-particle interactions of the additives on the flow

The effect of inter-particles interaction and finite aspect ratio of the additive are studied in this section. Figure (8) shows the influence of each one of these effects for $\varepsilon = 1.5$ and $\phi = 0.001$.

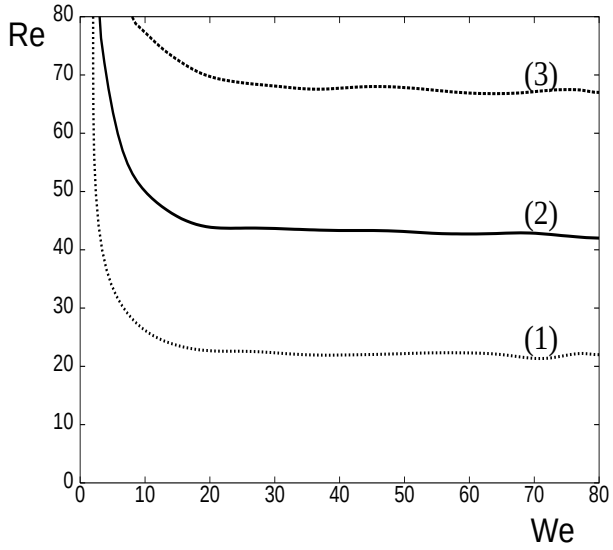

Figure 8: Influence of geometrical parameters of the additives on the collapse diagram for $\varepsilon = 1.5$ and $\phi = 0.1\%$. (1) shows the inter-particle interaction; (2) is the collapse diagram without any correction model; (3) finite aspect ratio influence.

In this plot, line (1) corresponds to the collapse diagram for inter-particle interaction; line (2) shows the diagram without these effects and line (3) corresponds to the effect of a finite aspect ratio. It is seen that

the interaction between two particles reduces the non-collapse region. A possible explanation for this is that the effect on the extensional viscosity produced by a additive orientation is reduced due to the presence of the another. In this case, the tendency of alignment of the particles in the flow direction is disturbed by the presence of the others particles, reducing the contribution of one particle orientation on the stabilization of the bubble motion. A finite aspect ratio effect is a more realistic model than infinitely long additives. The increasing of the non-collapse region can be justified by the fact that finite particles are more uniformly distributed in the whole suspension.

5.3. Initially randomly oriented additives influence

Next, some results for the new formulation proposed in section 3.6 are shown. Only additives aligned in the radial direction of the flow has been considered. Now we consider a suspension with configuration of particles randomly oriented with the radial direction.

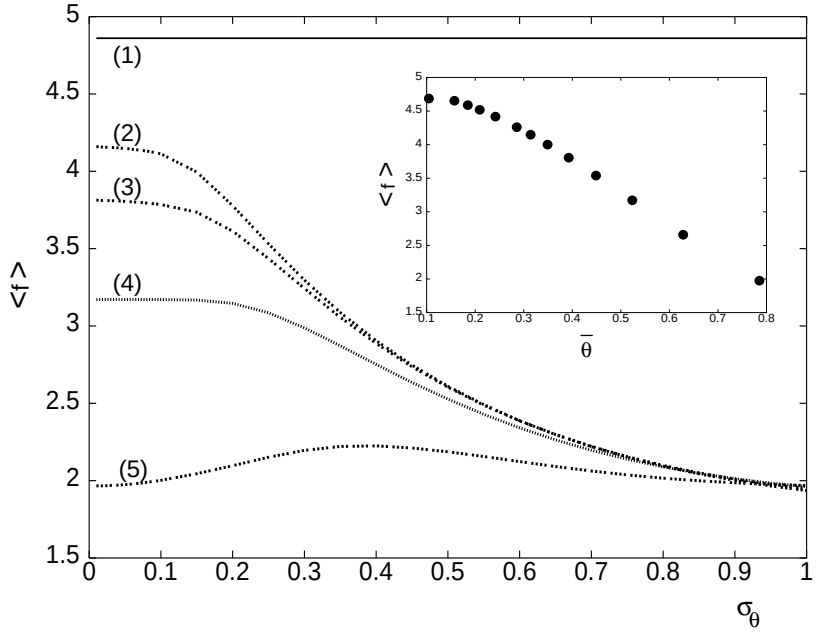

Figure 9: The average extensional rheological function for a normal probability density distribution . (1) Aligned additives; (2) $\bar{\theta} = \pi/10$; (3) $\bar{\theta} = \pi/8$; (4) $\bar{\theta} = \pi/6$; (5) $\bar{\theta} = \pi/4$. The insert in the figure shows $\langle f \rangle \times \bar{\theta}$ for a small standard deviation, $\sigma_\theta = 0.05$.

The plot in Fig. (9) shows the behavior of the rheology of the suspension as a function of the average angle of the additive orientation and its associated standard deviation. Notice that as the average orientation angle is smaller, for a small variance, the function $\langle f \rangle$ is nearly close to the corresponding particles orientation in the radial direction. As the average orientation angle is increased, the effect of the additives on the viscosity is reduced because only the normal component of the orientation of the particles in relation to the bubble wall acts on the extensional viscosity. A increasing in the standard deviation means that the particle can assume a greater range of orientation in the suspension. The plot shows that this increasing makes the rheological function tending asymptoticly to a value close to 2. The insert shows $\langle f \rangle \times \bar{\theta}$ for $\sigma_\theta = 0.05$. Notice that as the average angle moves away from the alignment condition the value of $\langle f \rangle$ decreases.

Figure (10) shows a comparison between the two models. Here, the parameters of the system for a suspension of $\phi = 0.001$ and aspect ratio equal to 100 are: $We = 7$; $Re = 7$ and the pressure amplitude 1.5. Figure (10.a) presents the temporal evolution of the bubble radius for both models, and Fig. (10.b) is the phase diagram. An interesting finding is that the stabilization effect on the system of randomly oriented additives is significantly reduced in comparing with the model of radial aligned particles. It can be seen that the amplitude difference is greater than 10%. The phase diagram confirms that the new model contributes less to the stabilization of the nonlinear bubble oscillations than the indicate also oriented additives.

In Fig. (11), the influence of the random orientation of the additives in the collapse diagram is presented. In this plot the lowest critical curve represents the collapse line in a flow without additives. It is seen that the non-collapse region for the model of randomly oriented additives has a smaller effect in comparison to the case of initial aligned additives model.

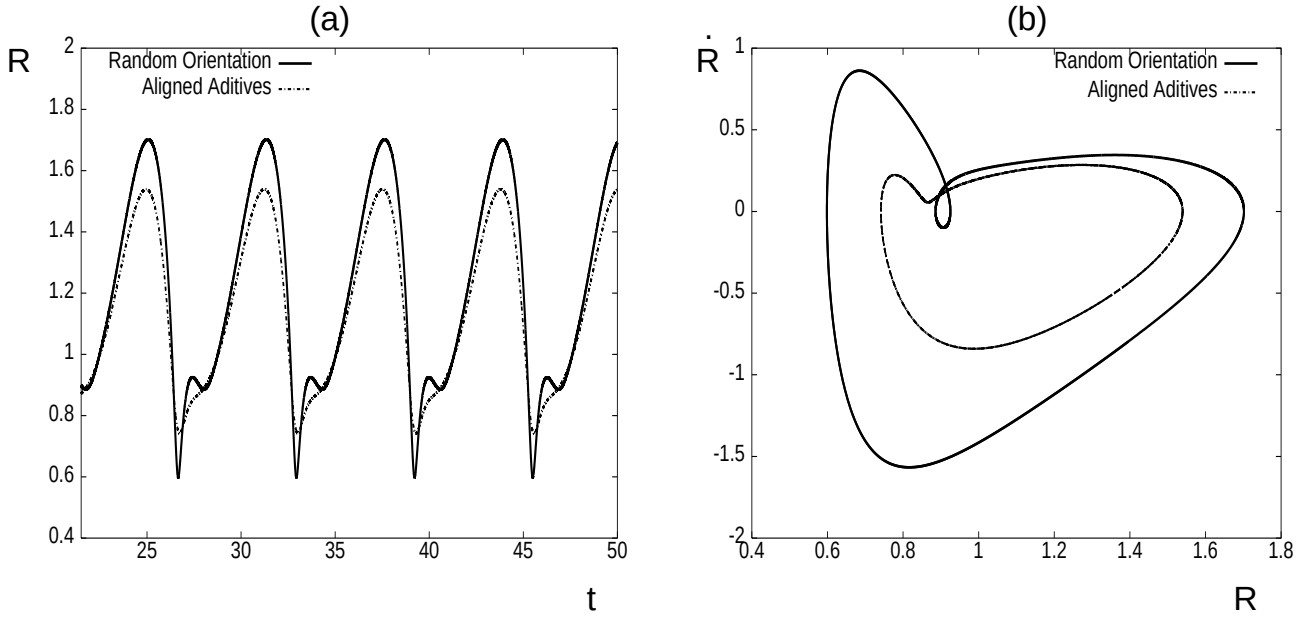

Figure 10: Comparison between the model of full aligned additives in the radial direction (full line) and the model of initially randomly oriented particles (dashed line) for $P(\theta) = N(\pi/6, 0.15)$. $\phi = 0.1\%$. (a) $R \times t$, (b) $\dot{R} \times R$

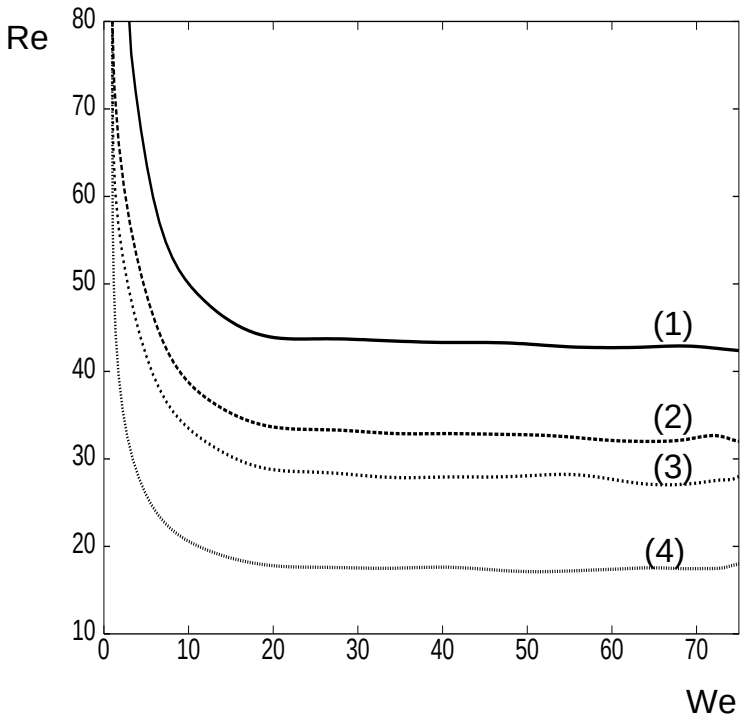

Figure 11: Comparison between collapse diagrams of random oriented additives model and the model of additives aligned to the radial motion of the bubble. $\varepsilon = 1.5$. (1) Aligned additives; (2) Random orientation for $P(\theta) = N(\pi/8; 0.15)$; (3) Random orientation for $P(\theta) = N(\pi/6; 0.15)$; (4) Random orientation for $P(\theta) = N(\pi/50; 0.9$.

6. Conclusion

The influence of additives on the behavior of a bubble under a acoustic pressure field has been analyzed in this work. It could be seen that bubble dynamics may be a severe unstable problem and in some cases the bubble collapses. The great amount of energy accumulated in a small volume of a collapsed bubble may cause serious damages in engineering process and, generally, cannot be avoided. The addition of particles, such as long fibers or macromolecule of polymers, can stabilize the flow even for critical situation like bubble collapse.

Bifurcations has been shown in the phase diagram. This plot has confirmed that when a small concentration of additives is used the flow tends to be stabilized. The influence of surface tension effects (We); viscous effects (Re) and the effect of the geometrical parameters of the additives (ϕ and ℓ/a) has been described by collapse diagrams. Small increasing on the concentration of particles or aspect ratio increase the domain influence of the non-collapse region. The system is more sensitive to Re than to We.

It could be observed that the model of aligned additives gives a stronger contribution on the stabilization of the bubble motion than the more realistic model of additives oriented randomly in the suspension. Inter-particles interaction and finite aspect ratio showed that some corrections to become the model more realistic may influence in different ways the system.

In concluding, the models adopted in this work show that addition of particles in a fluid can change drastically the nonlinear response of a bubble under acoustic cavitation.

7. References

Barber, B. P., Hiller, R. A., Lofsdedt, R., Putterman, R., and Weninger, K. R., 1997, Defining the Unknown of Sonoluminescence, "Phys. Reports", Vol. 281, pp. 80–82.

Batchelor, G. K., 1970, Slender-Body Theory for Particle of Arbitrary Cross Section in Stokes Flow, "J. Fluid Mech", Vol. 44, pp. 419.

Batchelor, G. K., 1971, The Stress Generated in a non-Dilute Suspension of Elongation Particles by Pure Straining, "J. Fluid Mech", Vol. 46, pp. 419.

Besant, W. H., 1859, "Hydrostatics and Hydrodynamics", Deighton Bell, Cambridge, Great Britain.

Blake, J. R. and Gibson, D. C., 1987, Cavitation Bubbles Near Boundaries, "Ann. Rev. of Fluid Mech.", Vol. 19, pp. 99–123.

Cheng, H. C. and Chen, L. H., 1986, Growth of a Gas Bubble in a Viscous Fluid, "Phys. Fluids(Series 6)", Vol. 29, pp. 3530–3536.

Hammit, F. G., 1980, "Cavitation and Multiphase Flow Phenomena", Ed. McGraw-Hill, New York, United States.

Hao, Y. and Prosperetti, A., 1999, The Dynamics of Vapor Bubbles in Acoustic Pressure Fields, "Phys. Fluids", Vol. 11, pp. 2008–2019.

Hinch, E. J. and Cunha, F. R., 1997, A Course on the Behavior of Elastic Liquids, University of Brasília - Department of Mechanical Engineering, pp 1-24.

Hinch, E. J. and Leal, L. G., 1970, Constitutive Equations in Suspension Mechanics. Part 2: Approximate Form for Suspension of Rigid Particles Effect by Brownian Motion, "J. Fluid Tech.", Vol. 73, pp. 187–208.

Kameth, V. and Prosperetti, A., 1989, A Numerical Integration Methods in Gas-Bubble Dynamics, "J. Acoust. Soc. Am.", Vol. 85, pp. 1538–1548.

Knapp, R., Daily, J., and Hammit, F., 1970, "Cavitation", Ed. McGraw-Hill.

Plesset, M. S. and Prosperetti, A., 1977, Bubble Dynamics and Cavitation, "Ann. Review of Fluid Mech.", Vol. 9, pp. 145–185.

Rayleigh, L., 1917, On the Pressure Developed in a Liquid During the Collapse of a Spherical Cavity, "Phil. Magazine", Vol. 34, pp. 94–98.

Santos, R. A. M. and Cunha, F. R., 2001, The Dynamic Behavior of a Collapsing Bubble in non-Newtonian Fluid, "Proceedings of the 16th Brazilian Congress of Mechanical Engineering", Vol. 1, pp. 510–519 (Section Fluid Mechanics), Uberlândia, Brazil.

Shaqfeh, E. S. G. and Frederickson, G. H., 1990, The Hydrodynamics Stress in a Suspension of Rods, "Phys. Fluids", Vol. 2, pp. 7–24.

Szeri, A. J. and Leal, L. G., 1991, The Onset of Chaotic Oscillations and Rapid Growth of a Spherical Bubble at Subcritical Conditions in an Incompressible Liquid, "Phys. of Fluids", Vol. A3, pp. 551–555.

Young, F. R., 1989, "Cavitation", Mc Graw Hill Book Company, Oxford, Great Britain.